Penerbit Akademia Baru

Journal of Advanced Research in Micro and Nano Engineering

Journal homepage:
https://www.akademiabaru.com/submit/index.php/armne/index
ISSN: 2756-8210

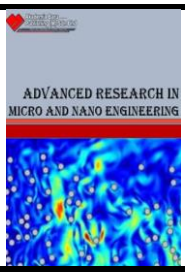

Influence of Calcination Temperature on the Physicochemical Properties of Synthesized Hydroxyapatite from Cow Bone Waste

Adibah Haneem Mohamad Dom[1,*], Salman Rezadin[1], Toibah Abd Rahim[1], Zurina Shamsudin[1], Siti Rahmah Shamsuri[1], Fahad Hussain Alhamoudi[2]

[1] Fakulti Teknologi dan Kejuruteraan Industri dan Pembuatan, Universiti Teknikal Malaysia Melaka, Hang Tuah Jaya, 76100, Durian Tunggal, Melaka, Malaysia
[2] Department of Allied Dental Health Science, College of Applied Medical Sciences, King Khalid University, Abha, 62529, Saudi Arabia

ARTICLE INFO

Article history:
Received 29 May 2024
Received in revised form 5 July 2024
Accepted 14 August 2024
Available online 30 September 2024

Keywords:

Hydroxyapatite; cow bone waste; cost-effective; thermal treatment; environmental impact

ABSTRACT

The chemical similarity found in hydroxyapatite (HA) with natural bone makes it a popular choice for bone replacement. Therefore, in recent years, there has been an increasing tendency towards manufacturing HA from biological sources or waste, such as animal bone waste. Using naturally derived HA can benefit the economy, the environment, and human health. Therefore, this paper reports on the extraction of HA from cow bone waste using a simple and cost-effective technique. The bone powder was calcined in a furnace at temperatures ranging from 700°C to 1000°C for two hours. Then, the synthesized HA was characterized using a Field Emission Scanning Electron Microscope (FESEM), Energy Dispersive X-ray Spectroscopy (EDX), Fourier Transform Infrared Spectroscopy (FTIR), and X-ray diffraction (XRD). FESEM images revealed that HA particles with non-uniform spherical morphology were produced where the size increases with the calcination temperature. This finding is consistent with the average value of particle diameter measured at a temperature of 1000°C (0.783±0.268 µm) which is much greater than at a temperature of 700°C (0.272±0.128 µm). EDX analysis revealed that the Ca/P ratio value obtained in this study indicates non-stoichiometric HA production. XRD analysis shows that only the HA phase is present and there is no secondary phase generated from the calcination process. Meanwhile, FTIR analysis can detect the main group elements of the HA which were OH^- and PO_4^{3-}. The findings obtained in this study prove the effectiveness of this method in producing highly crystalline HA powder from cow bone waste using the thermal treatment method.

1. Introduction

The increasing rate of urbanisation and industrialization has created considerable challenges for waste management and environmental protection [1]. Biological wastes necessitate the use of specific methods for disposal due to their pathogenicity, fluid content, and high oxidation rates. Proper waste processing can increase earnings from by-products simultaneously promoting environmental sustainability. The slaughterhouses are the largest sources of animal waste; a large

* *Corresponding author.*
E-mail address: adibah@utem.edu.my

https://doi.org/10.37934/armne.23.1.115127

part of these wastes cannot be transformed into value-added products. Examples of waste from the slaughterhouse are bones, skins, feathers, tendons, internal organs, and blood where this waste varies according to the food culture of each region [2].

In recent years, a range of sectors have initiated programs to address the issue of "food waste" [3]. Thus, researchers are increasingly investigating and valorising biogenic resources such as bio-waste to produce hydroxyapatite. Hydroxyapatite (HA), a member of the calcium phosphate family with the chemical formula $Ca_{10}(PO_4)_6(OH)_2$, is regarded as one of the most suitable bioceramics materials because of its biocompatibility, non-toxicity, osteointegration, and osteoconduction properties [4]. The ability of HA to stimulate bone regeneration and biological attachment with host tissue in the absence of supplements is due to the chemical and structure similarities [5,6]. HA will release Ca^{2+} and PO_3^{4-} ions when it is exposed to biological fluid and this in turn will help to promote cell proliferation and bone metabolism [7].

Due to its bioactivity, metallic implants such as titanium and stainless steel are frequently coated with HA [8,9]. This will help to enhance osteointegration and lower the implant rejection rate. In addition, HA can also be used in parts that have voids or bone defects. For that purpose, HA either in the form of powder, blocks, or beads will be placed in the affected bone area.

Numerous chemical methods such as wet chemical precipitation [10,11], hydrothermal synthesis [12,13], mechanochemical reaction [14,15], and sol-gel [16,17] methods have been widely employed to produce synthetic HA which is considered superior to those developed from natural sources [18]. However several disadvantages observed with the majority of these methods are intricate, expensive, and deficient in some essential trace elements [4,19]. Furthermore, most of the techniques that have been used to produce HA are only capable of producing it in small quantities [20]. In addition, the resulting HA often contains a second phase, beta-tricalcium phosphate (β-TCP) [21]. The formation of the β-TCP phase in the production of biomedical HA should be avoided due to its disadvantages [22,23]. Therefore, there is an ongoing effort to upgrade the process to bulk processing of highly crystalline HA.

In recent years, HA generated from natural sources, such as xenogeneic bone, has grown in popularity due to various advantages, including cost-effectiveness and environmentally friendly approaches, as well as sustainability due to its broad availability [24-26]. This will boost both the economy and general health. The present work describes the process of converting cow bone waste to HA powder using a simple thermal treatment method. The influence of calcination temperatures on the physicochemical properties of the obtained HA powders was characterised using Field Emission Scanning Electron Microscope (FESEM), Energy Dispersive X-ray Spectroscopy (EDX), Fourier Transform Infrared Spectroscopy (FTIR), and X-ray Diffraction (XRD).

2. Methodology

2.1 Synthesis of HA Powder from Cow Bone Waste

Waste cow bones as shown in Figure 1(a) which consist of various parts of the cow were collected from a local market in Batu Berendam, Malacca. The ends of the bones alongside the marrow and spongy areas were removed. Then, the bones were cleaned and boiled in boiling water for 2 hours to remove organic components and the adherent cow meats from the bones. Then, the cleaned bones were dried in an oven at 110 °C for 6 hours (Figure 1(b)).

The dried bones were cut into smaller pieces and crushed using mortar and pestle followed by milling using a planetary ball mill at 400 rpm for 3 hours to obtain bone powder form. Then, the dried bone powders were subjected to calcination treatment as shown in Figure 1(c). This calcination process is expected to effectively remove organic substances and kill pathogens [27].

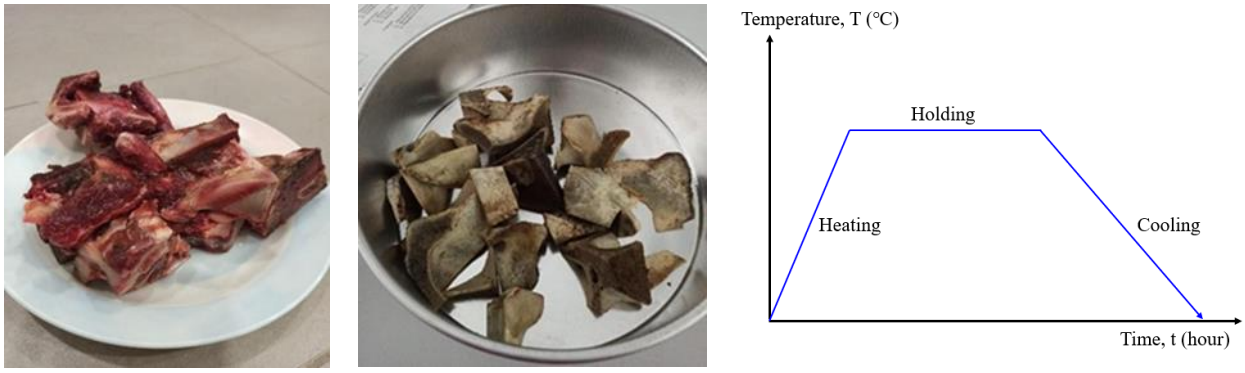

(a) (b) (c)

Fig. 1. (a)Waste cow bones, (b) dried cow bones and (c) schematic of thermal treatment to produce HA from cow bone waste

The calcination process was conducted in a furnace (Naberthem) at temperatures of 700, 800, 900, and 1000°C for 2 hours with the heating rate of 10°C per minute and left to cool in the furnace. The temperature selection is based on the findings by Manalu, Soegijono, and Indrani [25]. There are similarities in the XRD patterns obtained from beef bones calcined between 700–1000 °C with HA (JCPDS-09-0432). This finding shows that the HA produced at this temperature range has high purity and does not contain organic parts, making it suitable for biomedical applications.

2.2 Physicochemical Characterisation of HA Powder

Morphological analysis of all HA samples obtained at various calcination temperatures was carried out using a Field Emission Scanning Electron Microscope (FESEM, Hitachi SU 5000*).* The morphological observation was performed at 20000X magnification and 10 kV acceleration voltages. Before the analysis, each sample was fixed on a copper specimen holder with carbon tape and coated with platinum to make them conductive before testing. The average diameter of the synthesized particles was measured using ImageJ software where ten measurements were performed to obtain the average size value.

The elemental composition of the produced powder was identified by an EDX detector mounted on the FESEM machine. EDX analysis was performed at 15kV and a magnification of 15000X. The Ca/P ratio value for each sample was calculated as the average of four points used for EDX analysis.

The Rigaku MiniFlex 600 is a benchtop X-ray diffractometer that was employed to characterize the phase composition, crystallite sizes, and crystallinity of the synthesized HA samples. The X-ray

diffractometer was operated at an accelerating voltage of 40 kV and a current of 15 mA. A scan speed of 10 degrees/minute and a 0.02˚ step size were used to record data from 20 to 70°. The obtained XRD patterns were compared with standard reference to the HA (JCPDS 09–0432) pattern available in the X'Pert HighScore Plus software for phase identification.

Additionally, the crystallite size was calculated using the Scherrer equation shown in Eq. (1) [28]

$$d = \frac{K\lambda}{FWHM\ \cos\theta} \tag{1}$$

where, *d* is the crystallite diameter (nm), *K* is the shape constant (~0.9), λ is the X-ray beam wavelength (λ= 0.15406 nm), *FWHM* is the observed peak width at half- maximum peak height in radian and θ is the Bragg angle in degrees.

Meanwhile, the crystallinity index was evaluated from Eq. (2) [29] using the OriginPro software, which involves dividing the crystalline peak area by the overall area of the peaks.

$$\text{Crystallinity index} = \frac{\text{Area of all the crystalline peaks}}{\text{Area of all the crystalline and amorphous peaks}} \tag{2}$$

The functional groups of the prepared samples were determined by Fourier-transform infrared (FTIR) spectroscopy using a Jasco FTIR-6100 spectrometer. All powder samples were characterized using the ATR sampling method, where a spectrum of each sample was acquired in the wavenumber range from 400–4000 cm^{-1} at a spectral resolution of 4 cm^{-1}.

3. Results

3.1 Morphology of the Synthesised HA Powders

Figure 2 presents the FESEM images of the synthesised HA powder obtained after calcination at various temperatures. It can be observed that irregular spherical particle shapes with highly agglomerated particles of nanoparticles were produced at all temperatures. It is also visible from the images in Figure 2 that the particle size increases as the calcination temperature increases. To confirm this observation, ImageJ software was employed to measure the average particle diameter. Figure 3 presents the average diameter value taken from 10 measurements. The average diameter of the particles synthesised at 700, 800, 900, and 1000 °C were 0.272±0.128, 0.386±0.078, 0.544±0.155, and 0.783±0.268 µm, respectively.

Compared to the research conducted by Manalu, Soegijono, and Indrani [25], HA produced from cow bone waste has particle sizes of 0.416 and 0.833 µm at calcination temperatures of 700 and 900 °C, respectively. This indicates that the HA generated in this study is smaller in size than in previous research [22]. Smaller HA particle size is more beneficial because it increases the contact surface area of HA with the adjacent tissue when in application [30]. This will increase the interaction of HA surface, bone surface, and protein absorption in forming bone growth.

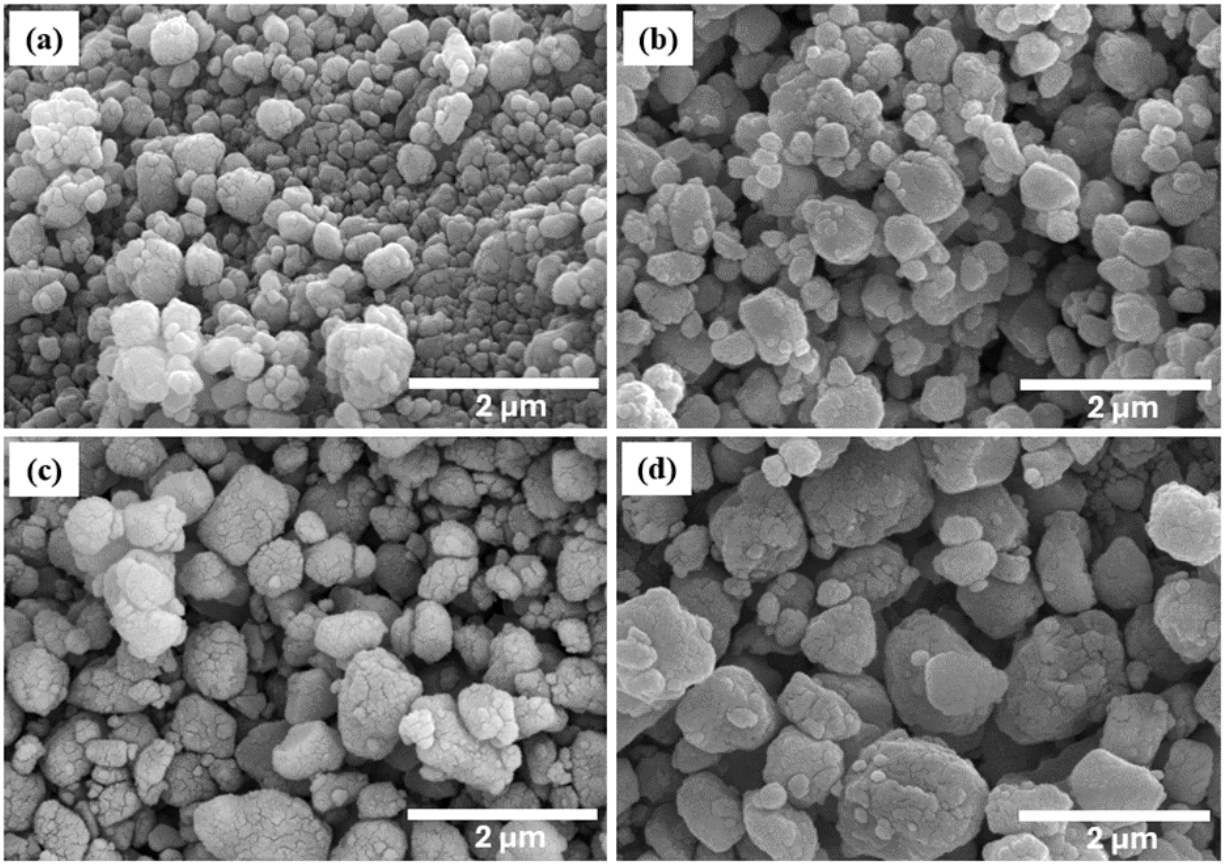

Fig. 2. FESEM images of the synthesised HA powder calcined at various temperatures; (a) 700 °C (b) 800 °C (c) 900 °C and (d) 1000 °C

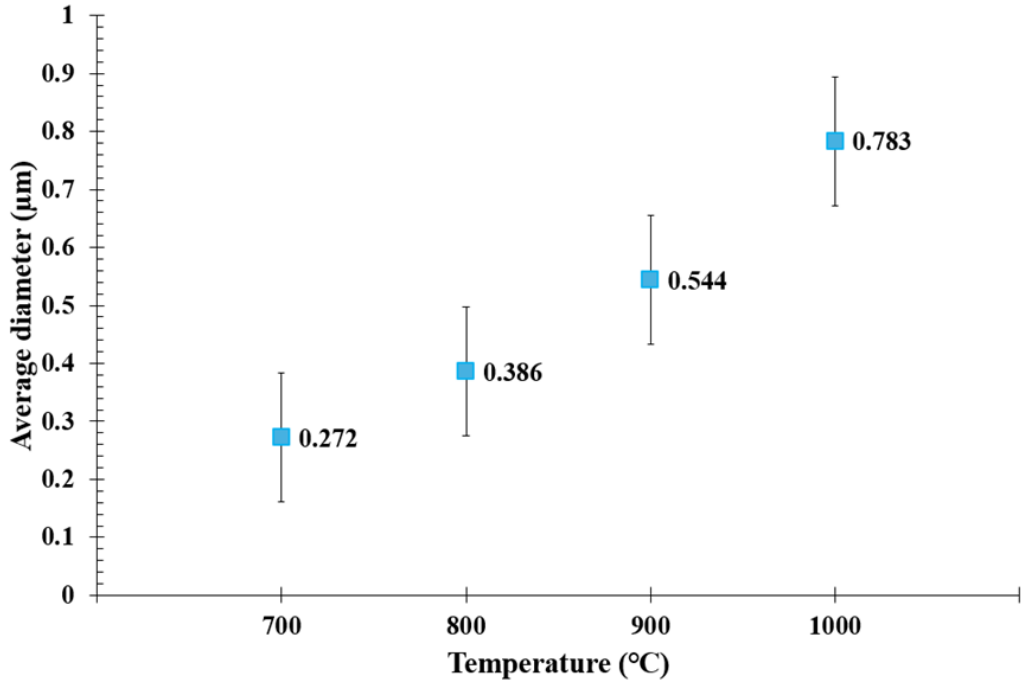

Fig. 3. Average diameter at various temperatures measured using the ImageJ software

An increase in the size of non-uniform spherical particle morphology was observed with increasing temperature. It is expected that at high temperatures, particles will continue to grow due to the lack of barriers (such as solutes, impurities, grain boundaries, etc.) that can prevent particle growth [31]. Thus, a suitable temperature should be selected to control the powder particle growth and hinder the occurrence of particle agglomeration.

Wu *et al.,* [32] reported a similar finding when they ground eggshell waste with dicalcium phosphate dihydrate (DCPD) for 1 hour and heated it at 1200 °C for 1 hour to produce HA powder. It was found that as the heating temperature increased from 900 to 1200 °C, the HA particles grew gradually where the average size increased from 1.62 to 2.54 µm.

One of the factors that caused the agglomeration of nanoparticles is the high Van der Waals forces formed between the particles [33,34]. Van der Waals forces refer to the weak forces that contribute to intermolecular bonding in solid materials. Agglomeration normally occurs when the attractive Van der Waals forces overcome the repulsion of the nanoparticles. Additionally, small particle size exhibits a greater attractive force. Therefore, the tendency of nanoparticles to agglomerate is higher as compared to the micro-size particles. As mentioned by Mishra and Ramaprabhu [35], nanoparticles are prone to easy agglomeration, which can substantially alter the reactivity, dispersion, and toxicity of the powder by modifying surface properties.

3.2 Elemental Composition Analysis

Elemental analysis of HA powder produced at various calcination temperatures is shown in Figure 4. It can be observed that calcium and phosphorus elements are present in all samples. From the atomic percentages obtained from EDX analysis, the Ca/P ratio can be calculated. Figure 5 shows the Ca/P ratio, showing a decrease with increasing calcination temperature. Additionally, the Ca/P ratio values obtained deviate from the stoichiometric HA ratio (Ca/P = 1.67) due to the presence of various beneficial elements in cow bone, which substitute calcium and phosphate ions in the apatite lattice. It is expected that some phosphate ions have been replaced by carbonate ions, resulting in the obtained Ca/P ratio being higher than the stoichiometric value of 1.67.

Nevertheless, the presence of these elements can also enhance the biological activity of HA produced from organic sources [36], as it more closely resembles apatite found in human bones. Despite the difference in Ca/P ratio compared to the stoichiometric value of HA, all ratios obtained fall within the acceptable range for HA, which is less than 2 [37].

The findings presented above are consistent with other studies that produced HA from cow bone waste using the calcination method. For instance, Ramesh *et al.,* [38] obtained HA with a Ca/P ratio ranging from 1.58 to 1.88, with the highest ratio observed at the lowest temperature of 600 °C. Meanwhile, Luthfiyah *et al.,* [39] obtained HA with a Ca/P ratio of 1.69 and 1.61 for temperatures of 850 and 900 °C. From these studies, it was found that the Ca/P ratio decreased with increasing calcination temperature, which is consistent with the trend observed in the current research.

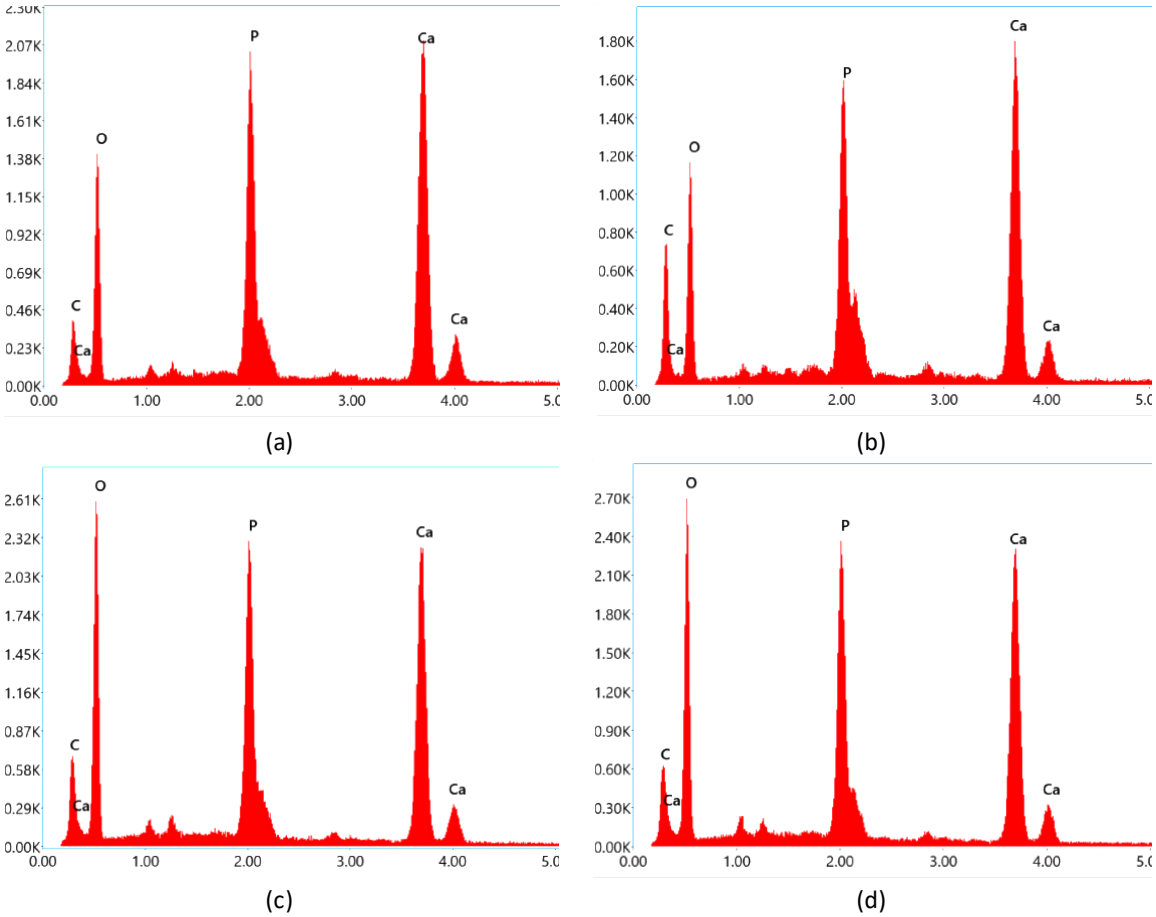

Fig. 4. The elemental analysis performed on the produced HA powder at various calcination temperatures (a) 700 °C (b) 800 °C (c) 900 °C and (d) 1000 °C

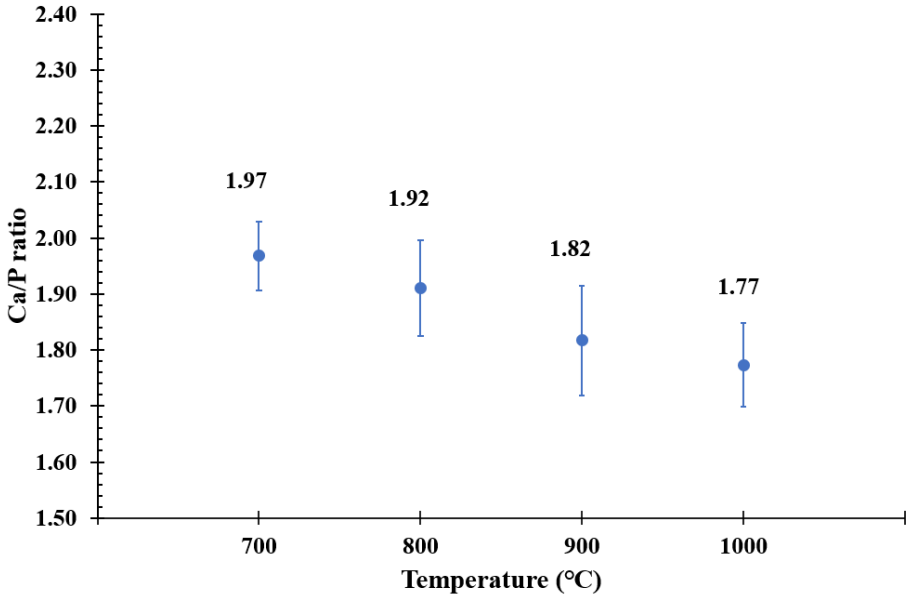

Fig. 5. Effect of temperature increment on the Ca/P ratio of the produced HA powder

3.3 FTIR Analysis

Figure 6 presents the FTIR spectra of the synthesised HA at various temperatures obtained in this study. The positions of the OH^- peak and the four vibration modes of PO_4^{3-} groups ($\nu_1, \nu_2, \nu_3, \nu_4$) were found to be consistent with findings from other studies [40, 41]. The OH^- peak is observed in all samples at approximately 3570 cm^{-1}. Two phosphate bands were identified at around 960 cm^{-1} and 470 cm^{-1}, corresponding to the ν_1 (symmetric stretching) and ν_2 (bending) modes, respectively. In the spectral region ~1087-1033 cm^{-1}, the ν_3 mode phosphate group (asymmetric stretching) also appears in all samples.

Two prominent peaks at 570 and 600 cm^{-1} indicate the ν_4 (bending) mode. Well-separated ν_4 peaks corresponding to transverse and longitudinal optical frequencies were evident in all samples, suggesting highly crystalline samples were successfully obtained [42]. In contrast, amorphous calcium phosphate would exhibit a broad single absorption band in this region due to structural lattice distortion. As HA transitions to a more crystalline state, its hexagonal structure becomes more pronounced. Consequently, the vibrational mode of PO_4^{3-} in this region splits into two distinct peaks, indicating increased crystallinity.

In addition to the OH^- and PO_4^{3-} vibrational peaks, the FTIR spectrum also shows carbonate bands at 1455–1464 cm^{-1} and ~875 cm^{-1}. The presence of the peak at 875 cm^{-1} suggests that some of the phosphate groups in the apatite structure have been replaced by carbonates [36]. This substitution is supported by previous EDX results where the Ca/P ratio obtained was higher than the stoichiometric HA ratio. The presence of carbonates in cow bones, as well as the absorption of carbon dioxide from the atmosphere during sample preparation, contributes to carbonate formation [43]. Carbonate is an important component of human bone structure, and its presence increases the bioactivity of HA [44]. However, their presence can also pose risks by potentially reducing the thermal stability of HA.

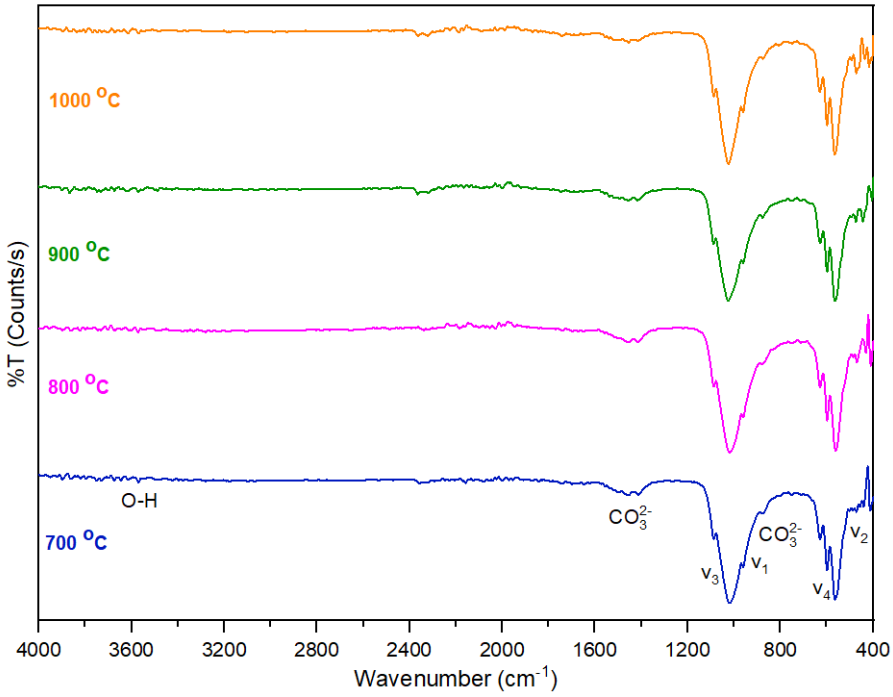

Fig. 6. FTIR spectra of the waste cow bone heated at various temperatures for 2 hours

3.4 Phase Composition and Crystallinity Analysis

Figure 7 depicts the XRD patterns of the HA powder after heat treatment at various temperatures as well as the HA reference pattern (JCPDS 09-0432). It was evident that there is a resemblance in the peak position of HA implying a good match between the reference and the synthesized pattern. Peaks correlated with the HA phase are in the range of 2θ = 25°–35° and can be observed in the XRD patterns (Figure 7). Only the HA phase is present, indicating that this method is effective in producing high purity HA.

Besides, no trace of other HA decomposition products, such as tricalcium phosphate (β-TCP) or tetra-calcium phosphate (TTCP) phases, was visible in the patterns. This also indicates that high crystalline HA was synthesized which can be evidenced by the appearance of the very sharp diffraction peaks of the XRD patterns. Also, it is apparent that with increasing temperatures, the peak intensity increases indicating the high crystallinity observed at high temperature. These intensity changes can be observed at the following peaks (002), (210), and (202). Apart from crystallinity, the extremely sharp diffraction peaks of the patterns also suggest that the HA powders with large crystallite sizes were produced using this method.

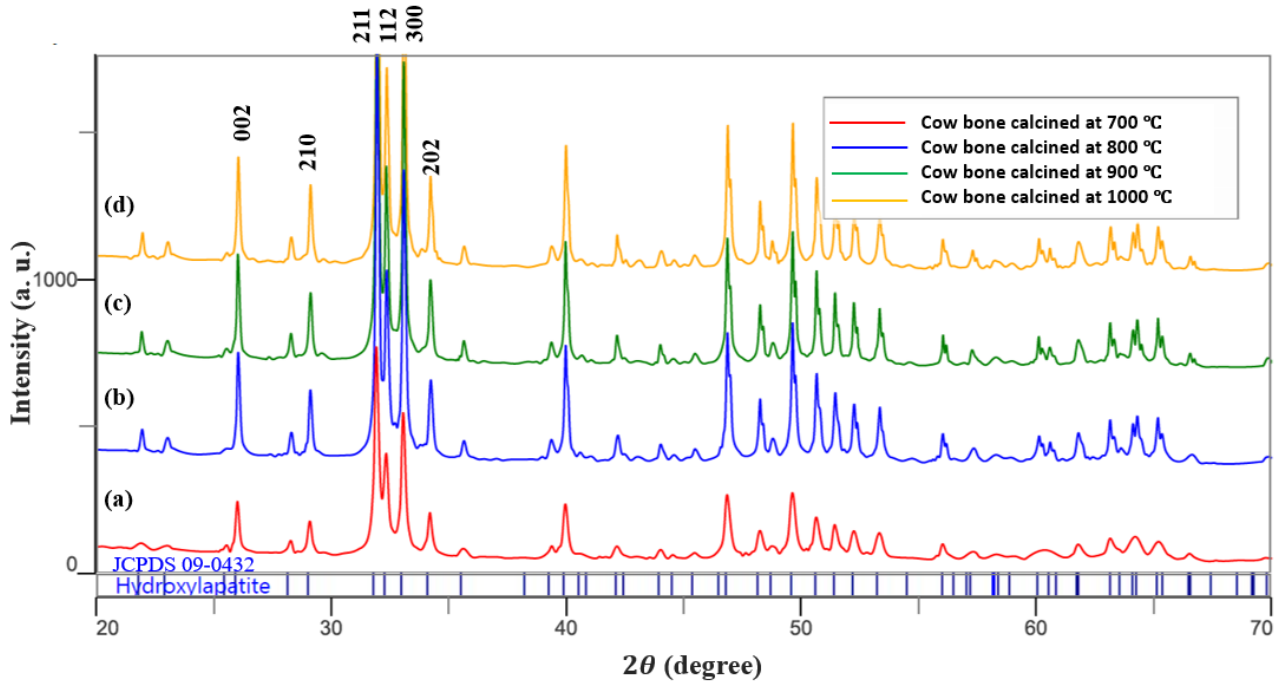

Fig. 7. The XRD patterns of the extracted HA obtained at various calcination temperatures (a) 700 ℃ (b) 800 ℃ (c) 900 ℃ and (d) 1000 ℃

The impact of heat treatment on crystallite growth and coarsening was validated by evaluating their sizes using the Scherrer equation. The average crystallite sizes recorded at 700, 800, 900, and 1000 °C were 55.94, 72, 78.27, and 79.59 nm, respectively (Table 1). It is clear that the heating at elevated temperatures leads to the generation of larger particles. This finding can be supported by the FESEM analysis, where small particles were observed after heating at 700 °C (Figure 2(a)), whereas heating at 1000 °C produces the largest particle (Figure 2(d)).

The effect of temperature increments on the crystallinity index can be observed from the data shown in Table 1. The crystallinity index rises with the gradual removal of amorphous phases, and the improvement of the crystalline structure occurs with increasing calcination temperature. Additionally, there is a tendency for the material's crystallinity to rise in tandem with an increase in

crystallite size. This is evidenced by the fact that HA powder calcined at 1000 °C had the largest crystallite size and highest crystallinity index value. It is expected that when the calcination temperature increases, the crystal size also increases due to the occurrence of crystal growth and the transformation of small crystals into larger ones. This change in size will also cause crystallinity to increase.

Table 1
Crystallite size and crystallinity index of the extracted HA

Temperature (°C)	FWHM		Crystallite size (nm)		Average size (nm)	Crystallinity index (%)
	(211)	(300)	(211)	(300)		
700	0.148	0.161	58.10	53.78	55.94	55.87
800	0.115	0.125	75.01	68.99	72.00	60.55
900	0.108	0.112	79.50	77.04	78.27	61.99
1000	0.105	0.112	82.00	77.18	79.59	70.3

4. Conclusions

Pure hydroxyapatite was successfully synthesised from cow bone waste using the thermal treatment method. The following conclusions can be gained based on the detailed analysis of the samples produced in this study:

i. Non-uniform spherical HA powders with highly aggregated particles made from nanoparticles were produced at all calcination temperatures. Increasing the calcination temperature causes the formation of larger particles. The average diameter of the particles calcined at a temperature of 700 °C is 0.272±0.128 µm and increases to 0.783±0.268 µm when the calcination temperature is 1000 °C.
ii. In addition, there is a decrease in the Ca/P ratio as the calcination temperature increases. The difference between the Ca/P ratio value obtained and the stoichiometric value of HA is due to the replacement of PO_4^{3-} ions in the HA structure.
iii. Meanwhile, XRD analysis showed the production of highly crystalline HA powder, in which only the HA phase was formed at all temperatures.
iv. The findings obtained in this study prove the feasibility of this material recycling technology in the conversion of cow bone waste into valuable HA.

Acknowledgement
Special acknowledgement to the Fakulti Teknologi dan Kejuruteraan Industri dan Pembuatan (FTKIP), Universiti Teknikal Malaysia Melaka (UTeM) for providing the facilities. This research was not funded by any grant.

References
[1] P Vijayaraghavan, MA Rathi, Khalid S Almaary, Fatima S Alkhattaf, Yahya B Elbadawi, Soon Woong Chang, and Balasubramani Ravindran. "Preparation and antibacterial application of hydroxyapatite doped Silver nanoparticles derived from chicken bone." *Journal of King Saud University-Science* 34, no. 2 (2022): 101749. https://doi.org/10.1016/j.jksus.2021.101749
[2] Birendra B Adhikari, Michael Chae, and David C Bressler. "Utilization of slaughterhouse waste in value-added applications: Recent advances in the development of wood adhesives." *Polymers* 10, no. 2 (2018): 176. https://doi.org/10.3390/polym10020176
[3] C Martin-Rios, A Hofmann, and N Mackenzie, *Sustainability-Oriented Innovations in Food Waste Management Technology. Sustainability 2021, 13, 210*. 2020. https://doi.org/10.3390/su13010210

[4] Mayank Kumar Yadav, Riddhi Hiren Shukla, and KG Prashanth. "A comprehensive review on development of waste derived hydroxyapatite (HAp) for tissue engineering application." *Materials Today: Proceedings* (2023): https://doi.org/10.1016/j.matpr.2023.04.669

[5] Gareth Turnbull, Jon Clarke, Frédéric Picard, Philip Riches, Luanluan Jia, Fengxuan Han, Bin Li, and Wenmiao Shu. "3D bioactive composite scaffolds for bone tissue engineering." *Bioactive materials* 3, no. 3 (2018): 278-314. https://doi.org/10.1016/j.bioactmat.2017.10.001

[6] Pooneh Kia, Mansor Bin Ahmad, and Kamyar Shameli. "Green synthesis of Sodium alginate mediated Fluorapatite Nanoparticle via Sol-Gel method." *Journal of Research in Nanoscience and Nanotechnology* 2, no. 1 (2021): 30-41. https://doi.org/10.37934/jrnn.2.1.3041

[7] Vivekanand Sabanna Kattimani, Sudheer Kondaka, and Krishna Prasad Lingamaneni. "Hydroxyapatite—Past, present, and future in bone regeneration." *Bone and Tissue Regeneration Insights* 7 (2016): BTRI. S36138. https://doi.org/10.4137/btri.s36138

[8] Daniel ArcosMaría Vallet-Regí. "Substituted hydroxyapatite coatings of bone implants." *Journal of Materials Chemistry B* 8, no. 9 (2020): 1781-1800. https://doi.org/10.1039/c9tb02710f

[9] Shikha Awasthi, Sarvesh Kumar Pandey, E Arunan, and Chandan Srivastava. "A review on hydroxyapatite coatings for the biomedical applications: experimental and theoretical perspectives." *Journal of Materials Chemistry B* 9, no. 2 (2021): 228-249. https://doi.org/10.1039/d0tb02407d

[10] Azade Yelten-YilmazSuat Yilmaz. "Wet chemical precipitation synthesis of hydroxyapatite (HA) powders." *Ceramics International* 44, no. 8 (2018): 9703-9710. https://doi.org/10.1016/j.ceramint.2018.02.201

[11] Omar M Gomez-Vazquez, Brandon A Correa-Piña, Luis F Zubieta-Otero, Angelica M Castillo-Paz, Sandra M Londoño-Restrepo, and Mario E Rodriguez-García. "Synthesis and characterization of bioinspired nano-hydroxyapatite by wet chemical precipitation." *Ceramics International* 47, no. 23 (2021): 32775-32785. https://doi.org/10.1016/j.ceramint.2021.08.174

[12] Masahiro YoshimuraHiroyuki Suda, *Hydrothermal processing of hydroxyapatite: past, present, and future*, in *Hydroxyapatite and related materials*. 2017, CRC press. p. 45-72. https://doi.org/10.1201/9780203751367-3

[13] Shahid HussainKazi Sabiruddin. "Effect of reaction time on the phase quantity of hydroxyapatite synthesized from Indian clam seashell by hydrothermal technique." *Journal of the Australian Ceramic Society* 60, no. 2 (2024): 419-434. https://doi.org/10.1007/s41779-023-00948-x

[14] Nudthakarn Kosachan, Angkhana Jaroenworaluck, Sirithan Jiemsirilers, Supatra Jinawath, and Ron Stevens. "Hydroxyapatite nanoparticles formed under a wet mechanochemical method." *Journal of Biomedical Materials Research Part B: Applied Biomaterials* 105, no. 3 (2017): 679-688. https://doi.org/10.1002/jbm.b.33590

[15] MV Chaikina, NV Bulina, I Yu Prosanov, OB Vinokurova, and AV Ishchenko. "Structure formation of zinc-substituted hydroxyapatite during mechanochemical synthesis." *Inorganic Materials* 56 (2020): 402-408. https://doi.org/10.1134/s0020168520040044

[16] OA Osuchukwu, A Salihi, I Abdullahi, and DO Obada. "Synthesis and characterization of sol–gel derived hydroxyapatite from a novel mix of two natural biowastes and their potentials for biomedical applications." *Materials Today: Proceedings* 62 (2022): 4182-4187. https://doi.org/10.1016/j.matpr.2022.04.696

[17] Mahin Baladi, Mahnaz Amiri, Parisa Mohammadi, Karrar Salih Mahdi, Zahra Golshani, Razieh Razavi, and Masoud Salavati-Niasari. "Green sol–gel synthesis of hydroxyapatite nanoparticles using lemon extract as capping agent and investigation of its anticancer activity against human cancer cell lines (T98, and SHSY5)." *Arabian Journal of Chemistry* 16, no. 4 (2023): 104646. https://doi.org/10.1016/j.arabjc.2023.104646

[18] NAS Mohd Pu'ad, RH Abdul Haq, H Mohd Noh, HZ Abdullah, MI Idris, and TC Lee. "Synthesis method of hydroxyapatite: A review." *Materials Today: Proceedings* 29 (2020): 233-239. https://doi.org/10.1016/j.matpr.2020.05.536

[19] Deepak K Pattanayak, Rajalaxmi Dash, RC Prasad, BT Rao, and TR Rama Mohan. "Synthesis and sintered properties evaluation of calcium phosphate ceramics." *Materials Science and Engineering: C* 27, no. 4 (2007): 684-690. https://doi.org/10.1016/j.msec.2006.06.021
[20] A Ruksudjarit, K Pengpat, G Rujijanagul, and T Tunkasiri. "Synthesis and characterization of nanocrystalline hydroxyapatite from natural bovine bone." *Current applied physics* 8, no. 3-4 (2008): 270-272. https://doi.org/10.1016/j.cap.2007.10.076
[21] Decky J Indrani, Bambang Soegijono, Wisnu A Adi, and Neil Trout. "Phase composition and crystallinity of hydroxyapatite with various heat treatment temperatures." *Int. J. Appl. Pharm* 9, no. 2 (2017): 87-91. https://doi.org/10.22159/ijap.2017.v9s2.21
[22] UK Nahar, B Shovon, RD Chandra, B Shukanta, and SP Chandra. "Characterization of beta-tricalcium phosphate (β-TCP) produced at different process conditions." *J Bioengineer & Biomedical Sci* 7, no. 221 (2017): 2. https://doi.org/10.4172/2155-9538.1000221
[23] Marc Bohner, Bastien Le Gars Santoni, and Nicola Döbelin. "β-tricalcium phosphate for bone substitution: Synthesis and properties." *Acta biomaterialia* 113 (2020): 23-41. https://doi.org/10.1016/j.actbio.2020.06.022
[24] Krzysztof Haberko, Mirosław M Bućko, Jadwiga Brzezińska-Miecznik, Maria Haberko, Włodzimierz Mozgawa, Tomasz Panz, Anna Pyda, and Jerzy Zarębski. "Natural hydroxyapatite —its behaviour during heat treatment." *Journal of the European Ceramic Society* 26, no. 4-5 (2006): 537-542. https://doi.org/10.1016/j.jeurceramsoc.2005.07.033
[25] Jojorlamsihar Manalu, Bambang Soegijono, and Decky Jusiana Indrani. "Characterization of hydroxyapatite derived from bovine bone." *Asian Journal of Applied Sciences* 3, no. 4 (2015): https://doi.org/10.22159/ijap.2017.v9s2.21
[26] Zaharah Abdul Rahman, Sofiah Hamzah, Syed Mohd Saufi Tuan Chik, Norhafiza Ilyana Yatim, Siti Solihah Rasdei, and Jan Setiawan. "Properties and Evaluation of Functionalized Mixed Membrane Adsorbents for the Adsorption of Vanillic Acid from Palm Oil Waste." *Journal of Advanced Research in Applied Sciences and Engineering Technology* 39, no. 2 (2024): 53-71. https://doi.org/10.37934/araset.39.2.5371
[27] Muhammad Akram, Rashid Ahmed, Imran Shakir, Wan Aini Wan Ibrahim, and Rafaqat Hussain. "Extracting hydroxyapatite and its precursors from natural resources." *Journal of materials science* 49 (2014): 1461-1475. https://doi.org/10.1007/s10853-013-7864-x
[28] AR Toibah, F Misran, A Shaaban, and Z Mustafa. "Effect of pH condition during hydrothermal synthesis on the properties of hydroxyapatite from eggshell waste." *Journal of Mechanical Engineering and Sciences* 13, no. 2 (2019): 4958-4969. https://doi.org/10.15282/jmes.13.2.2019.14.0411
[29] Alireza Noori, Mahdieh Hoseinpour, Sedighe Kolivand, Nasrin Lotfibakhshaiesh, Somayeh Ebrahimi-Barough, Jafar Ai, and Mahmoud Azami. "Exploring the various effects of Cu doping in hydroxyapatite nanoparticle." *Scientific Reports* 14, no. 1 (2024): 3421. https://doi.org/10.1038/s41598-024-53704-x
[30] Mingzu Du, Jingdi Chen, Kaihua Liu, Huaran Xing, and Cui Song. "Recent advances in biomedical engineering of nano-hydroxyapatite including dentistry, cancer treatment and bone repair." *Composites Part B: Engineering* 215 (2021): 108790. https://doi.org/10.1016/j.compositesb.2021.108790
[31] S Farag, I Konyashin, and B Ries. "The influence of grain growth inhibitors on the microstructure and properties of submicron, ultrafine and nano-structured hardmetals–A review." *International Journal of Refractory Metals and Hard Materials* 77 (2018): 12-30. https://doi.org/10.1016/j.ijrmhm.2018.07.003
[32] Shih-Ching Wu, Hsueh-Chuan Hsu, Shih-Kuang Hsu, Ya-Chu Chang, and Wen-Fu Ho. "Effects of heat treatment on the synthesis of hydroxyapatite from eggshell powders." *Ceramics International* 41, no. 9 (2015): 10718-10724. https://doi.org/10.1016/j.ceramint.2015.05.006
[33] Ilse Gosens, Jan Andries Post, Liset JJ de la Fonteyne, Eugene HJM Jansen, John W Geus, Flemming R Cassee, and Wim H de Jong. "Impact of agglomeration state of nano-and submicron sized gold particles on pulmonary inflammation." *Particle and fibre toxicology* 7, no. 1 (2010): 1-11. https://doi.org/10.1186/1743-8977-7-37

[34] Stefan Christian Endres, Lucio Colombi Ciacchi, and Lutz Mädler. "A review of contact force models between nanoparticles in agglomerates, aggregates, and films." *Journal of Aerosol Science* 153 (2021): 105719. https://doi.org/10.1016/j.jaerosci.2020.105719

[35] Ashish Kumar MishraSundara Ramaprabhu. "Palladium nanoparticles decorated graphite nanoplatelets for room temperature carbon dioxide adsorption." *Chemical Engineering Journal* 187 (2012): 10-15. https://doi.org/10.1016/j.cej.2011.01.024

[36] Edwin A Ofudje, Archana Rajendran, Abideen I Adeogun, Mopelola A Idowu, Sarafadeen O Kareem, and Deepak K Pattanayak. "Synthesis of organic derived hydroxyapatite scaffold from pig bone waste for tissue engineering applications." *Advanced Powder Technology* 29, no. 1 (2018): 1-8. https://doi.org/10.1016/j.apt.2017.09.008

[37] Nasser AM Barakat, Myung Seob Khil, AM Omran, Faheem A Sheikh, and Hak Yong Kim. "Extraction of pure natural hydroxyapatite from the bovine bones bio waste by three different methods." *Journal of materials processing technology* 209, no. 7 (2009): 3408-3415. https://doi.org/10.1016/j.jmatprotec.2008.07.040

[38] Singh Ramesh, Zi Zhen Loo, Chou Yong Tan, WJ Kelvin Chew, Yern Chee Ching, Faris Tarlochan, Hari Chandran, Sivakumar Krishnasamy, Le Thi Bang, and Ahmed AD Sarhan. "Characterization of biogenic hydroxyapatite derived from animal bones for biomedical applications." *Ceramics International* 44, no. 9 (2018): 10525-10530. https://doi.org/10.1016/j.ceramint.2018.03.072

[39] Syifa Luthfiyah, Bambang Soegijono, Ferry Budhi Susetyo, and Hamdan Akbar Notonegoro. "Comparing properties of bovine bone derived hydroxyapatite and synthetic hydroxyapatite." *Journal of Applied Science and Engineering* 25, no. 6 (2022): 1197-1203. https://doi.org/10.6180/jase.202212_25(6).0015

[40] Ihtesham RehmanW Bonfield. "Characterization of hydroxyapatite and carbonated apatite by photo acoustic FTIR spectroscopy." *Journal of Materials Science: Materials in Medicine* 8, no. 1 (1997): 1-4. https://doi.org/10.1023/a:1018570213546

[41] Sanosh Kunjalukkal Padmanabhan, Avinash Balakrishnan, Min-Cheol Chu, Yong Jin Lee, Taik Nam Kim, and Seong-Jai Cho. "Sol–gel synthesis and characterization of hydroxyapatite nanorods." *Particuology* 7, no. 6 (2009): 466-470. https://doi.org/10.1016/j.partic.2009.06.008

[42] GM Poralan, JE Gambe, EM Alcantara, and RM Vequizo. *X-ray diffraction and infrared spectroscopy analyses on the crystallinity of engineered biological hydroxyapatite for medical application*. in *IOP conference series: materials science and engineering*. 2015. IOP Publishing. https://doi.org/10.1088/1757-899x/79/1/012028

[43] Peipei Wang, Caihong Li, Haiyan Gong, Xuerong Jiang, Hongqiang Wang, and Kaixing Li. "Effects of synthesis conditions on the morphology of hydroxyapatite nanoparticles produced by wet chemical process." *Powder Technology* 203, no. 2 (2010): 315-321. https://doi.org/10.1016/j.powtec.2010.05.023

[44] Feray Bakan, Oral Lacin, and Hanifi Sarac. "A novel low temperature sol–gel synthesis process for thermally stable nano crystalline hydroxyapatite." *Powder Technology* 233 (2013): 295-302. https://doi.org/10.1016/j.powtec.2012.08.030